

1                   **Textile waste and microplastic induce activity and**  
2                   **development of unique hydrocarbon-degrading marine**  
3                   **bacterial communities**

4  
5 Elsa B. Girard<sup>1</sup>, Melanie Kaliwoda<sup>2</sup>, Wolfgang W. Schmahl<sup>1,2,3</sup>, Gert Wörheide<sup>1,3,4</sup> and

6 William D. Orsi<sup>1,3\*</sup>

7  
8 <sup>1</sup> Department of Earth and Environmental Sciences, Ludwig-Maximilians-Universität München,  
9 80333 Munich, Germany

10 <sup>2</sup> SNSB - Mineralogische Staatssammlung München, 80333 München, Germany

11 <sup>3</sup> GeoBio-Center<sup>LMU</sup>, Ludwig-Maximilians-Universität München, 80333 Munich, Germany

12 <sup>4</sup> SNSB - Bayerische Staatssammlung für Paläontologie und Geologie, 80333 Munich, Germany

13 \*Corresponding author (e-mail: [w.orsi@lrz.uni-muenchen.de](mailto:w.orsi@lrz.uni-muenchen.de))

14  
15  
16  
17  
18 **KEYWORDS**

19 Microplastic, Fiber, Hydrocarbon-degrading bacteria, Microbial community, Pollution

20

21

## 22 **ABSTRACT**

23 Biofilm-forming microbial communities on plastics and textile fibers are of growing interest since  
24 they have potential to contribute to disease outbreaks and material biodegradability in the  
25 environment. Knowledge on microbial colonization of pollutants in the marine realm is expanding,  
26 but metabolic responses during substrate colonization remains poorly understood. Here, we assess  
27 the metabolic response in marine microbial communities to three different micropollutants, virgin  
28 high-density polyethylene (HDPE) microbeads, polysorbate-20 (Tween), and textile fibers.  
29 Intertidal textile fibers, mainly cotton, virgin HDPE, and Tween induced variable levels of  
30 microbial growth, respiration, and community assembly in controlled microcosm experiments.  
31 RAMAN characterization of the chemical composition of the textile waste fibers and high-  
32 throughput DNA sequencing data shows how the increased metabolic stimulation and  
33 biodegradation is translated into selection processes ultimately manifested in different  
34 communities colonizing the different micropollutant substrates. The composition of the bacterial  
35 communities colonizing the substrates were significantly altered by micropollutant substrate type  
36 and light conditions. Bacterial taxa, closely related to the well-known hydrocarbonoclastic bacteria  
37 *Kordiimonas* spp. and *Alcanivorax* spp., were enriched in the presence of textile-waste. The  
38 findings demonstrate an increased metabolic response by marine hydrocarbon-degrading bacterial  
39 taxa in the presence of microplastics and textile waste, highlighting their biodegradation potential.  
40 The metabolic stimulation by the micropollutants was increased in the presence of light, possibly  
41 due to photochemical dissolution of the plastic into smaller bioavailable compounds. Our results  
42 suggest that the development and increased activity of these unique microbial communities likely  
43 play a role in the bioremediation of the relatively long lived textile and microplastic pollutants in  
44 marine habitats.

45

## 46 **INTRODUCTION**

47 Plastics are synthetic organic polymers that are composed of long chains of monomers primarily  
48 made from petrochemical sources <sup>1</sup>. The mismanagement of waste in regions with high coastal  
49 population density has been linked to high plastic input into the ocean, resulting in an annual flow  
50 of 4.8 to 12.7 million tons per year since 2010 <sup>2</sup>. Once released in the environment, debris are

51 readily colonized by complex microbial communities<sup>3</sup>. Consequently, macro- and micro-litter  
52 may facilitate microbial dispersal throughout the marine realm. However, knowledge gaps  
53 regarding the mechanisms of microbial biodegradation of plastic and textile waste.

54 Plastic-degrading microorganisms have been studied since the 1960's. Summer studied the  
55 inhibition of microorganism growth for lasting polymers, to counter the deterioration of plastics  
56 due to mold and bacteria, because some plasticisers (chemical additives used to provide strength  
57 and flexibility), e.g., Ester-type plasticisers, are in turn a source of nutrients, which sustains  
58 microbial activity leading to natural degradation of the polymer<sup>4</sup>. More recent studies have shed  
59 some light on the diversity of microbial communities colonizing synthetic polymers. For example,  
60 Zettler *et al.* (2013) identified a highly diverse microbial community settled on plastic debris,  
61 termed as the “plastisphere”, unraveling polymer-dependent communities<sup>5</sup>. Moreover, its species  
62 richness appears to be more important than the microbial community in seawater samples for a  
63 given surface<sup>3,5</sup>. The colonization of plastic debris by bacteria is hypothesized as a two-step  
64 settlement: primary colonization by  $\alpha$ - and  $\gamma$ -proteobacteria, and subsequent secondary  
65 colonization by Bacteroidetes<sup>6,7</sup>.

66 Bioremediation of plastic pollution can be aided by heterotrophic bacteria<sup>8</sup>. These  
67 microorganisms may survive by extracting the carbon from plastic particles, via hydrolysis of the  
68 hydrocarbon polymer<sup>7,8</sup>. Recent studies have identified a few bacterial species able to deteriorate  
69 plastics, for example, *Ideonella sakainesis*, which is a betaproteobacterium actively degrading  
70 polyethylene (PE)<sup>9</sup>. The plastisphere also harbours a variety of potential pathogens, i.e., harmful  
71 microorganisms to animals, such as *Vibrio* spp.<sup>3,5,6</sup>. Indeed, Lamb *et al.* observed the transfer of  
72 harmful bacteria from plastic litter to reef-building corals, causing three diseases (skeletal eroding  
73 band disease, white syndromes and black band disease), which led to coral mortality<sup>10</sup>. Such  
74 observation highlights the need for reducing and taking action on plastic pollution in the  
75 environment.

76 Microparticles of textile waste (i.e., synthetic and natural fibers) enter the ocean due to  
77 atmospheric deposition and poor wastewater incubation plant filtration systems allowing the  
78 leakage of fibers to the aquatic environment, making it one of the most abundant and recorded  
79 micropollutants at sea<sup>11,12</sup>. Thus, this study aims to assess the potential for bioremediation of  
80 microplastics and textile waste by marine microbial communities in a controlled microcosm  
81 experiments.

82 The main questions addressed here are whether specific micropollutant-associated microbial  
83 communities develop in the presence of high-density polyethylene (HDPE) microbeads and textile  
84 fibers as sole source of carbon, and how these substrates influence their metabolic state.  
85 Furthermore, we investigated whether light has an impact on the development and metabolism of  
86 these communities. We hypothesized that hydrocarbon-degrading microbes can use microplastics  
87 and textile waste as the sole carbon source, and that different types of microplastics will select for  
88 unique communities with different levels of activity. Because light also plays a role in the abiotic  
89 degradation of organic matter in aquatic environments<sup>13</sup>, we hypothesized that exposure to light  
90 may also improve the ability of the bacteria to utilize carbon from plastic polymers as a growth  
91 substrate due to its photochemical dissolution. The results contribute to our understanding of the  
92 formation and development of plastics and textile-waste-associated microbes and their potential  
93 role in bioremediation of these widespread environmental micropollutants.

94  
95

## 96 MATERIAL AND METHODS

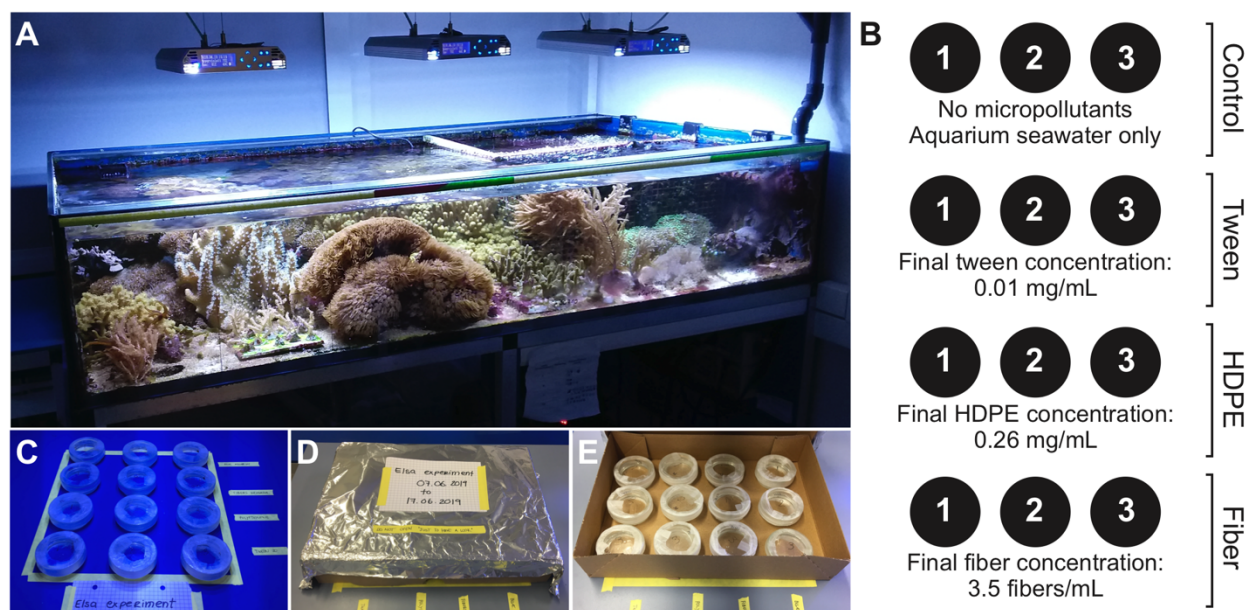
97

98 **Experimental setup and sampling.** A total of 15 mL of aquarium seawater containing  
99 microbial communities were incubated in 20 mL glass petri dishes for 108 h at room temperature,  
100 which received either no micropollutants (control), polysorbate (Tween) 20, Tween 20 and HDPE  
101 microbeads, or textile fibers (Tab. 1, Fig. 1). Tween 20 was used as a control since it is used as an  
102 emulsifier for the HDPE microbeads and thus serves to test whether the microbes respond only to  
103 the Tween or also are effected by the HDPE itself. The artificial seawater microbial community  
104 comes from an aquarium (642 L) built of imported live rocks, which hosts many reefs organisms,  
105 such as hexacorals, octacorals, gorgonians, sea anemones (*Aiptasia* sp.), marine sponges  
106 (*Lendenfeldia chondrodes*, *Tethya wilhelma*), marco-algae (*Chaetomorpha linum*) and  
107 cyanobacteria, mussels (*Mytilus edulis*) and benthic foraminifera (*Elphidium crispum*) (Fig. 1A).  
108 For each of these incubations, one set was placed under LEDs (Mitras LX6200 HV; light spectrum  
109 of 380 nm to 700 nm) with a 12/24 h light cycle (referred to as “light”) and the other one placed  
110 inside a cardboard box covered with aluminium foil to block incoming light (referred to as “dark”)  
111 (Fig. 1). Each incubation set consists of twelve glass petri dishes sealed with parafilm containing  
112 a submerged oxygen sensor spot (PreSens Precision Sensing): three controls and nine incubations

113 (Fig. 1B). The oxygen sensor spot was positioned at the bottom of the petri dish to measure the  
114 minimal concentration of O<sub>2</sub>, that could be dissolved into the bottom water of the petri dish after  
115 diffusion from the overlying headspace.

116 The oxygen concentration in each incubation was closely monitored over the first 48 h of the  
117 experiment using a Stand-alone Fiber Optic Oxygen Meter (PreSens Fibox 4) interacting with the  
118 oxygen sensor spots. At the beginning of the experiment, four samples of 15 mL were collected  
119 from the aquarium to assess the initial microbial community (T<sub>0</sub>; referred to as “aquarium”). All  
120 incubations and aquarium samples were processed through 4 or 15 mL Amicon® Ultra Centrifugal  
121 Filters (4000 rpm, RCF 3399 \*g, 10 min. at 20 °C) to concentrate microbes and associated particles  
122 depending on the incubation. The concentrated supernatant was equally transferred in two Lysing  
123 matrix E tubes for every incubation.

124



125

126 **Figure 1.** Experimental setup. A) Aquarium hosting a small reef ecosystem from which 15 mL was transferred  
127 into each incubation petri dish. B) incubation set of twelve glass petri dishes and associated incubations. C)  
128 Experimental display under artificial sunlight. D) and E) experimental display with limited access to light.

129

130

131

132

**Incubation      Description**

Control	Control petri dishes containing only 15 mL of artificial seawater, with no micropollutants.
Tween	0.1% Tween 20 solution produced following the solubilisation protocol of Cospheric LLC ( <a href="https://www.cospheric.com/">https://www.cospheric.com/</a> ).  150 $\mu$ L of tween solution was added to 15 mL of artificial seawater.  Final tween concentration: 0.01 mg/mL.
HDPE	Virgin HDPE microbeads (1-4 $\mu$ m; 0.96 g/cm <sup>3</sup> ) solubilized in 0.1% Tween 20 solution (final concentration of 2.6% solid solution of HDPE).  150 $\mu$ L of HDPE solution was added to 15 mL of artificial seawater.  Final HDPE concentration: 0.26 mg/mL.
Textile fiber	Ca. 500 textile fibers were collected from intertidal sediment at Coral Eye Resort (Bangka Island, North Sulawesi, Indonesia). Fibers were washed twice in Ethanol >99%.  150 $\mu$ L of Milli-Q H <sub>2</sub> O containing 50-60 fibers was added to 15 mL of artificial seawater.  Final fiber concentration: 3.5 fibers/mL.

133

134 **Table 1.** Description of each incubation type, equally exposed to light and dark conditions.

135

136 **Quantitative PCR.** The DNA was extracted as in Pichler *et al.* (2018), using 1 mL of a C1  
137 extraction buffer<sup>14</sup>. To lyse cells, the samples were subsequently heated at 99 °C for 2 min, frozen  
138 at -20 °C for 1 h, thawed at room temperature, and heated again at 99 °C for 2 min. After  
139 homogenization and centrifugation, the samples were concentrated a second time through Amicon  
140 filters, down to a final volume of ca. 100  $\mu$ L. The supernatant was purified following the DNeasy®  
141 PowerClean® Pro Cleanup Kit (Qiagen, Hilden, Germany). To assess the number of 16S copies  
142 at the end of the experiment, all samples were amplified using quantitative PCR (qPCR; Bio-Rad  
143 CFX connect™ Real-Time System). Every reaction contained 4 $\mu$ L of DNA template, 10  $\mu$ L of

144 Supermix, 5.2  $\mu\text{L}$   $\text{H}_2\text{O}$ , and 0.4  $\mu\text{L}$  of forward and reverse primer, and were subject to the following  
145 PCR program: denaturation at 95  $^\circ\text{C}$  for 3 min, and 40 amplification cycles (denaturation at 95  $^\circ\text{C}$   
146 for 10 s, annealing 55  $^\circ\text{C}$  for 30 s). All qPCR reactions were set up using an Eppendorf EpMotion  
147 pipetting robot that has <5% technical variation and results in qPCR reaction efficiencies (standard  
148 curves) having >90%<sup>15</sup>.

149

150 **16S amplicon library preparation.** To assess the diversity of the microbial community in the  
151 experimental samples, the V4 hypervariable region 16S rRNA gene (ca. 250 base pairs) was  
152 amplified with a set of primers (515F 5'-TATGGTAATTGTGTGCCAGCMGCCGCGGTAA-3'  
153 and 806R 5'-AGTCAGTCAGCCGGACTACHVGGGTWTCTAAT-3'), combined to a forward  
154 (P5) and reverse (P7) adaptor, and unique dual indices for every sample<sup>14</sup>. The preparation of the  
155 samples for the polymerase chain reaction (PCR) was done according to Pichler *et al.* (2018). In  
156 short, 4  $\mu\text{L}$  of extracted DNA was mixed to 5  $\mu\text{L}$  5x PCR buffer, 1  $\mu\text{L}$  50 mM dNTP, 1  $\mu\text{L}$  forward  
157 515F and 1  $\mu\text{L}$  reverse 806R primers, 9.9  $\mu\text{L}$   $\text{H}_2\text{O}$ , 3  $\mu\text{L}$   $\text{MgCl}_2$  and 0.1  $\mu\text{L}$  Taq DNA polymerase,  
158 for a total volume of 25  $\mu\text{L}$  for each sample. The amplification took place under specific PCR  
159 settings: denaturation at 95  $^\circ\text{C}$  for 3 min, 35 amplification cycles (denaturation at 95  $^\circ\text{C}$  for 10 s,  
160 annealing 55  $^\circ\text{C}$  for 30 s, elongation 72  $^\circ\text{C}$  for 1 min), and elongation at 72  $^\circ\text{C}$  for 5 min to ensure  
161 polymerization of all amplified DNA strands. PCR products were run through a 1.5% (w/v)  
162 agarose gel, and DNA strands were subsequently extracted using the QIAquick® Gel Extraction  
163 Kit (Qiagen, Hilden, Germany). The DNA concentration was quantified using the fluorometer  
164 QuBit 2.0 (Life Technologies, Grand Island, USA) and its associated dsDNA high-sensitivity  
165 assay kit. As preparation for 16S amplicon sequencing, all samples were pooled together by adding  
166 5  $\mu\text{L}$  of every sample at a DNA concentration of 1 nM.

167

168 **16S amplicon sequencing.** A high diversity library was added to the 16S amplicon pool to  
169 enhance the recognition of the 16S sequences by the Illumina MiniSeq. The DNA was denatured  
170 by adding of 0.1 nM NaOH for a short period of 5 min, which was then directly neutralized with  
171 a tris-HCl buffer (pH 7) to avoid hydrolyzation of the DNA. To not overload the flow cell, a two-  
172 step dilution was performed on the 16S pool for a final DNA concentration of 1.8 pM, resulting in  
173 a final volume of 500  $\mu\text{L}$  MiniSeq solution. Four additional sequencing primers after<sup>14</sup> were added  
174 to successfully undergo the dual-index barcoding with the MiniSeq. Finally, the prepared 1.8 pM

175 solution of 16S, transcriptomes, and the four sequencing primers was loaded into the reagent  
176 cartridge.

177  
178 **Data analysis.** To transform the demultiplexed sequences from Illumina MiniSeq into an OTU  
179 table, the raw data was manipulated using USEARCH v11.0 (<https://drive5.com/usearch>)<sup>16</sup>  
180 following the method developed by Pichler and colleagues (2018). Most similar sequences sharing  
181 at least 97% of bases were grouped, and associated to an operational taxonomic unit (OTU). Each  
182 OTU was classified within the Taxonomic Classification System using MacQiime v1.9.1  
183 (<http://qiime.org/>). To keep a control on the analyzed data, OTUs of less than 10 reads to all  
184 samples were discarded. Statistical analyses were computed in R v3.3.3<sup>17</sup>. For phylogenetic  
185 reconstruction, most abundant selected OTUs were identified using blastn (BLAST®,  
186 <https://blast.ncbi.nlm.nih.gov/>). Sequences were aligned in MAFFT v7.427 (<https://mafft.cbrc.jp/alignment/software/>). The phylogenetic tree was inferred using Seaview v4.7<sup>18</sup> under PhyML  
187 optimized settings (GTR model), including 100 bootstrap replicates<sup>19</sup>. All related primary data  
188 and R scripts are stored on GitHub (<https://github.com/PalMuc/PlasticsBacteria>).

190  
191 **Raman spectroscopy.** Forty textile fibers were randomly subsampled and their associated  
192 spectrum obtained with a HORIBA JOBIN YVON XploRa ONE micro Raman spectrometer  
193 belonging to the Mineralogical State Collection Munich (SNSB). The used Raman spectrometer  
194 is equipped with edge filters, a Peltier cooled CCD detector and three different lasers working at  
195 532 nm (green), 638 nm (red) and 785 nm (near IR). To perform the measurements the near IR  
196 Laser (785 nm) was used, with a long working distance objective (LWD), magnification 100x  
197 (Olympus, series LMPlanFL N), resulting in a 0.9  $\mu\text{m}$  laser spot size on the sample surface. The  
198 wavelength calibration of the IR laser was performed by manual calibration with a pure Si wafer  
199 chip, the main peak intensity had values in the interval  $520\text{ cm}^{-1} \pm 1\text{ cm}^{-1}$ . The wave number  
200 reproducibility was checked several times a day providing deviation of less than  $< 0.2\text{ cm}^{-1}$ .  
201 Monthly deviation was in the range of  $1\text{ cm}^{-1}$  before calibration. The necessary power to obtain a  
202 good-quality spectrum varied between 10% and 50% (i.e., respectively 2.98 mW and 18 mW  $\pm$   
203 0.1 mW on the sample surface) depending on the type and degraded stage of the measured textile  
204 fiber. The pin-hole and the slit were respectively set at 300 and 100. Each acquisition included two  
205 accumulations with a grading of 1200 T and an integration time of 5 s over a spectral range of 100



206 to 1600  $\text{cm}^{-1}$ . The precision of determining Raman peak positions by this method is estimated to  
207 be  $\pm 1$  to  $\pm 1.5$   $\text{cm}^{-1}$ . Resulting Raman spectra were analyzed using LabSpec Spectroscopy Suite  
208 software v5.93.20, treated in R v3.3.3, manually sorted in Adobe Illustrator CS3, and compared  
209 with available spectra from published work. All related Raman spectra and R scripts are stored on  
210 GitHub (<https://github.com/PalMuc/PlasticsBacteria>).

211

212

## 213 **RESULTS & DISCUSSION**

214

215 For four days, a coral reef aquarium microbial community was incubated with Tween 20, HDPE  
216 microbeads and intertidal textile fibers in a microcosm experiment to test its potential to  
217 bioremediate widespread micropollutants. After sequencing of the V4 hypervariable region of the  
218 16S rDNA genes a total of 1,463,028 sequences were obtained, from a total of 50 samples. After  
219 the quality control on the data, all sequences were clustered in 3,884 OTUs, of which 563 (85%)  
220 could be taxonomically classified.

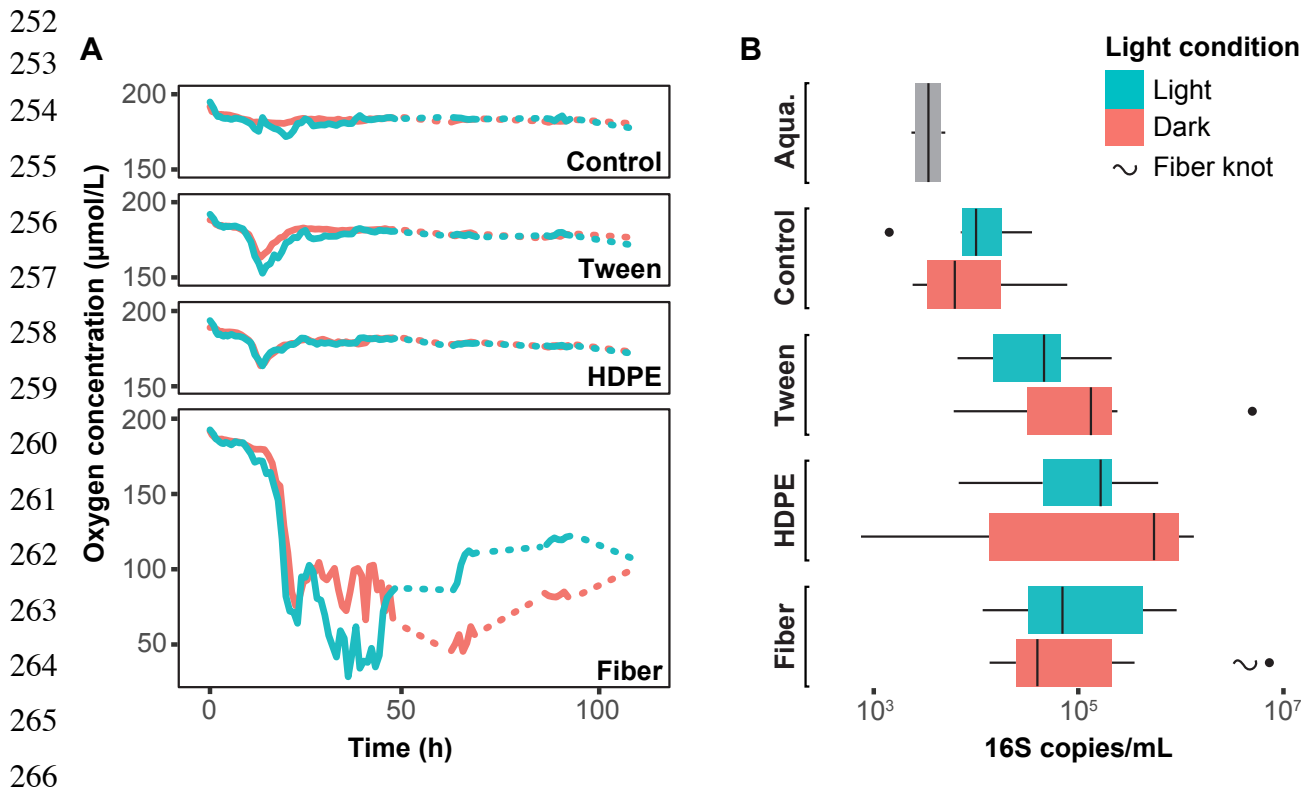
221

222 **Respiration and induced microbial activity.** Ten to 12 hours after the beginning of the  
223 experiment, a noticeable decrease in oxygen concentration was measured in all incubations  
224 containing micropollutants that was not observed in the control (Fig. 2A). This increased oxygen  
225 consumption in the presence of micropollutants indicates that microbial metabolism was  
226 stimulated by these pollutants, and their utilization as a carbon source for growth. It is likely that  
227 the transition between initial and final microbial communities initiated at this time in all  
228 incubations, which correlates with the theory that plastic surfaces are colonized within 24 h in the  
229 natural environment <sup>6</sup>.

230 Control, tween and HDPE incubations reached an equilibrium between oxygen consumption and  
231 production after this time, whereas microbial communities in the textile fiber incubations  
232 continued to consume oxygen at a high rate (Fig. 2A). This indicates a higher microbial activity  
233 induced by the intertidal textile fibers. These fibers were mainly pigmented with a black dye (CI.  
234 reactive black 5 or 8) and a blue dye (phthalocyanine 15 (PB15)) according to the Raman analysis  
235 <sup>20,21</sup>. Indeed, as much as 42% of the fiber spectra expressed only the fiber pigment, covering the  
236 fabric signal and preventing the identification of the polymer composition (Fig. 3). Here, only

237 cotton expressed a signal strong enough to be recognized in the Raman spectra, with characteristic  
 238 Raman peaks at positions 379, 435, 953, 1091 and 1116  $\text{cm}^{-1}$  (Fig. 3). Hence, at least 44% of all  
 239 fibers collected in the intertidal zone were identified as cotton, which appears to be one of the most  
 240 abundant fiber materials found in the environment <sup>11,22</sup>.

241 As textile fibers were sampled directly from an intertidal sandy beach in Indonesia (see Table  
 242 1), they were already exposed to high ultraviolet (UV) radiation and temperature, which are the  
 243 main factors participating in polymer degradation and fragmentation on beaches <sup>23-25</sup>. Indeed, UV  
 244 radiation causes photooxidative degradation, which results in breaking of the polymer chains,  
 245 produces free radicals and reduces the molecular weight, causing deterioration of the material,  
 246 after an unpredictable time <sup>26</sup>. This process rendered the textile fibers more subject to colonization  
 247 in comparison to virgin HDPE microbeads, due to their advanced deteriorated stage, and likely  
 248 facilitated the hydrolysis of carbon by hydrocarbon-degrading bacteria <sup>27</sup>. Another study, by  
 249 Romera-Castillo et al., demonstrated that irradiated plastic debris stimulated microbial activity in  
 250 a mesocosm experiment in comparison to virgin plastics, supporting the results obtained in our  
 251 study <sup>28</sup>.



266  
 267  
 268 **Figure 2.** A) Oxygen respiration measured in the four incubations (average of three replicates. Dashed lines represent  
 269 missing data (nights where no measurements were taken). B) 16S rRNA gene copies measured with qPCR in the same four  
 270 incubations at the end of the experiment. Error bars represent standard deviations across three biological replicate  
 271 incubations.

269

270

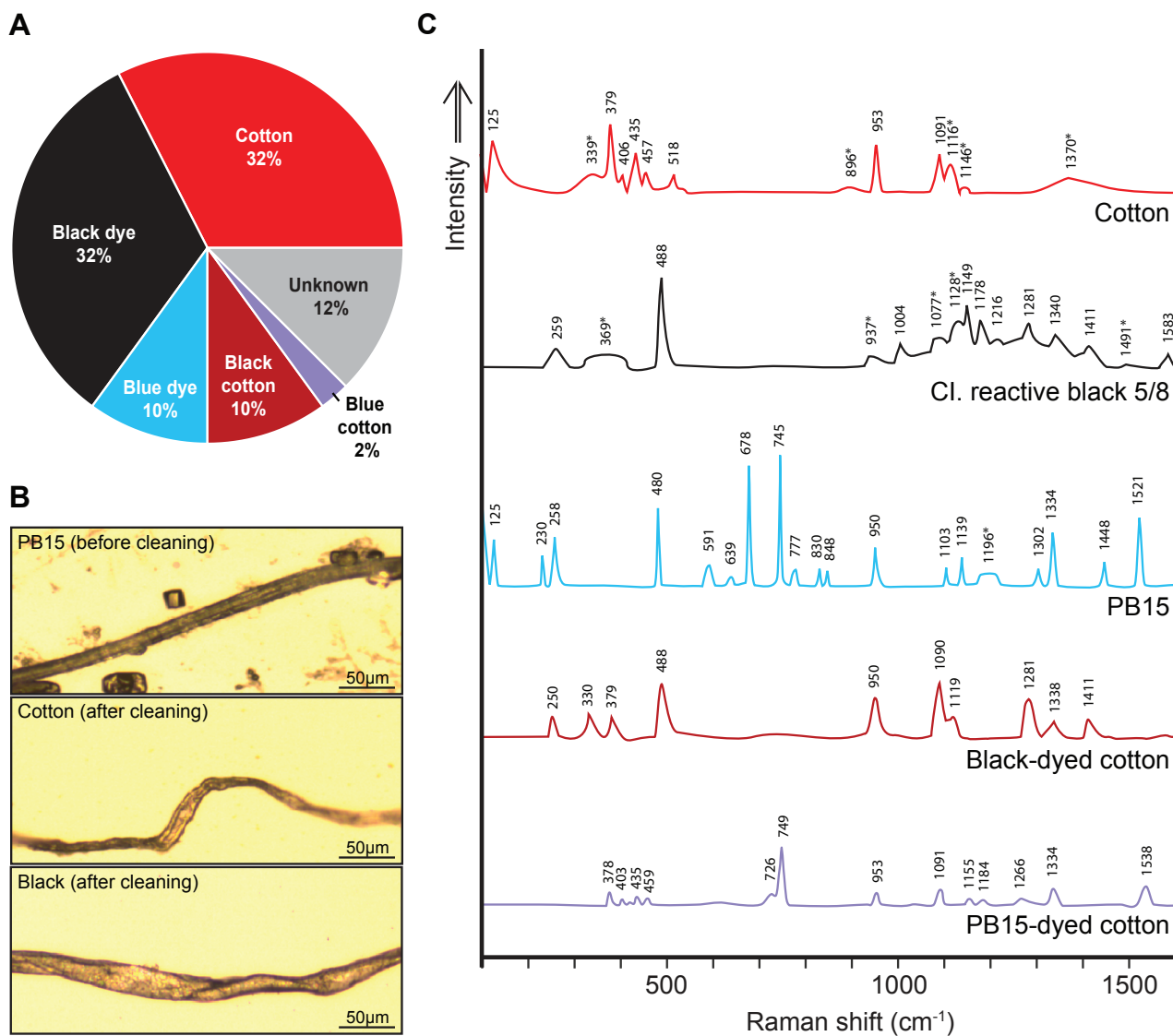


**Figure 3.** Analysis of the textile fiber sample extracted from the intertidal sediment at Coral Eye Resort. A) fiber type ratio based on signals obtained with Raman spectroscopy. B) photomicrographs of different fibers measured with Raman spectroscopy, illustrating examples of fibers before and after cleaning. C) Raman spectra of five fiber types identified. Numbers indicate the position of the peaks (cm<sup>-1</sup>) and the associated asterisk (\*) indicates a broad peak. Note: in 42% of the measurements, only the pigment signals were expressed, covering the polymer signature and preventing the identification of the fabric of those fibers. Only cotton seems to have a signal strong enough to overcome the pigment signature.

271

272

273

274 **Microbial community development.** Another indication that microbial communities developed  
275 according to the provided carbon source (i.e., tween, HDPE microbeads and intertidal textile  
276 fibers) is the higher amount of 16S copies in tween, HDPE and textile fiber incubations measured  
277 using qPCR, in comparison to the control incubations (Fig. 2B). Moreover, microbial communities  
278 were significantly different (Analysis of Similarity:  $P < 0.01$ ) between incubation types (Fig. 4),  
279 in comparison to the initial microbial community measure from the aquarium, which was  
280 dominated by the families Bacillaceae, Planctomycetaceae, Bacteriovoraceae and  
281 Cellvibrionaceae (Fig. 5).

282 Flavobacteriaceae and Vibrionaceae were particularly ubiquitous in control, tween and HDPE  
283 incubations. However, HDPE-incubated communities were enriched with bacteria from the Family  
284 Alcanivoraceae, whereas communities from the textile fiber incubations were enriched with

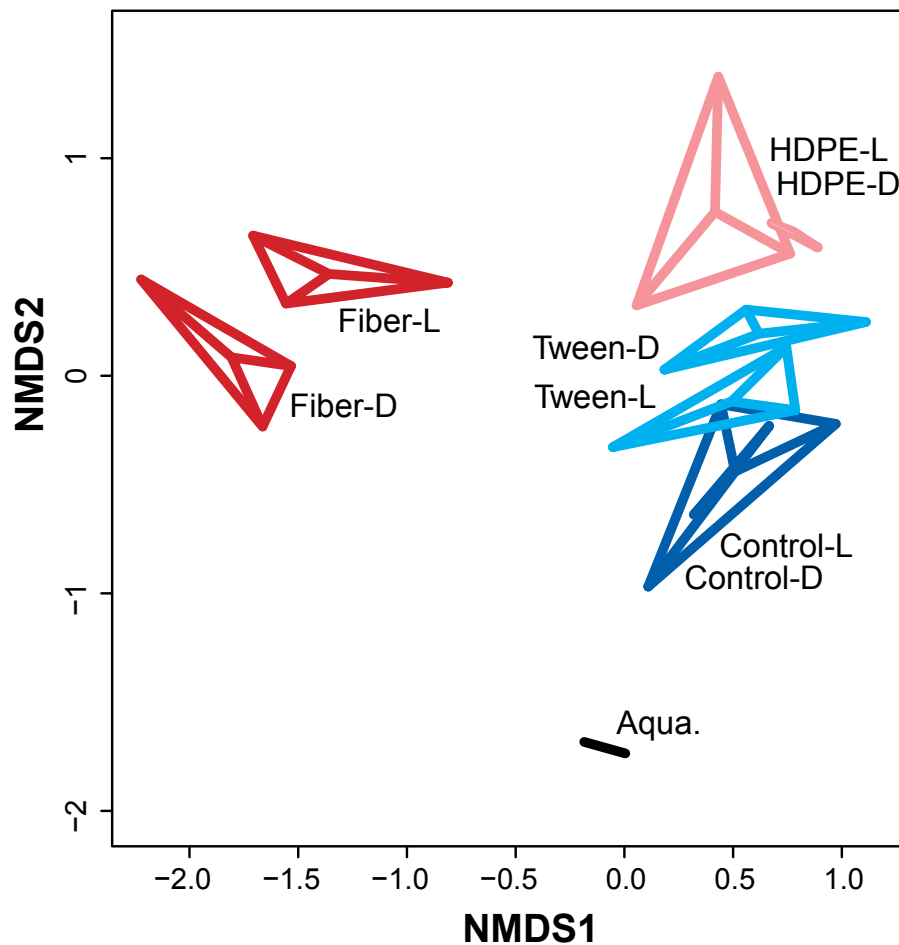


**Figure 4.** Non-metric multidimensional scaling (NMDS) analysis highlighting the difference in arbitrary distances between incubation-specific microbial communities (ANOSIM  $p = 0.001$ ).

285 bacteria from the Kordiimonadaceae and Cellvibrionaceae (Fig. 5). The observed difference  
 286 between microbial communities from micropollutant-bearing and control incubations might also  
 287 be explained by an accumulation of plastic-associated dissolved organic carbon (DOC) in the  
 288 microcosms<sup>28</sup>. Romera-Castillo et al. discovered that plastic debris releases a non-negligible  
 289 amount of DOC, most of it leaches within the first few days after the initial contact with seawater,  
 290 which would be applicable to the virgin HDPE microbeads<sup>28</sup>.

291 Control and tween incubations had a highly variable microbial communities between replicates,  
 292 whereas HDPE and textile fiber incubations showed very similar replicates. Nonetheless, all had  
 293 differences in the community composition between light and dark settings (Fig. 4, 5). The disparity  
 294 between microbial communities from incubations with HDPE microbeads and textile fibers

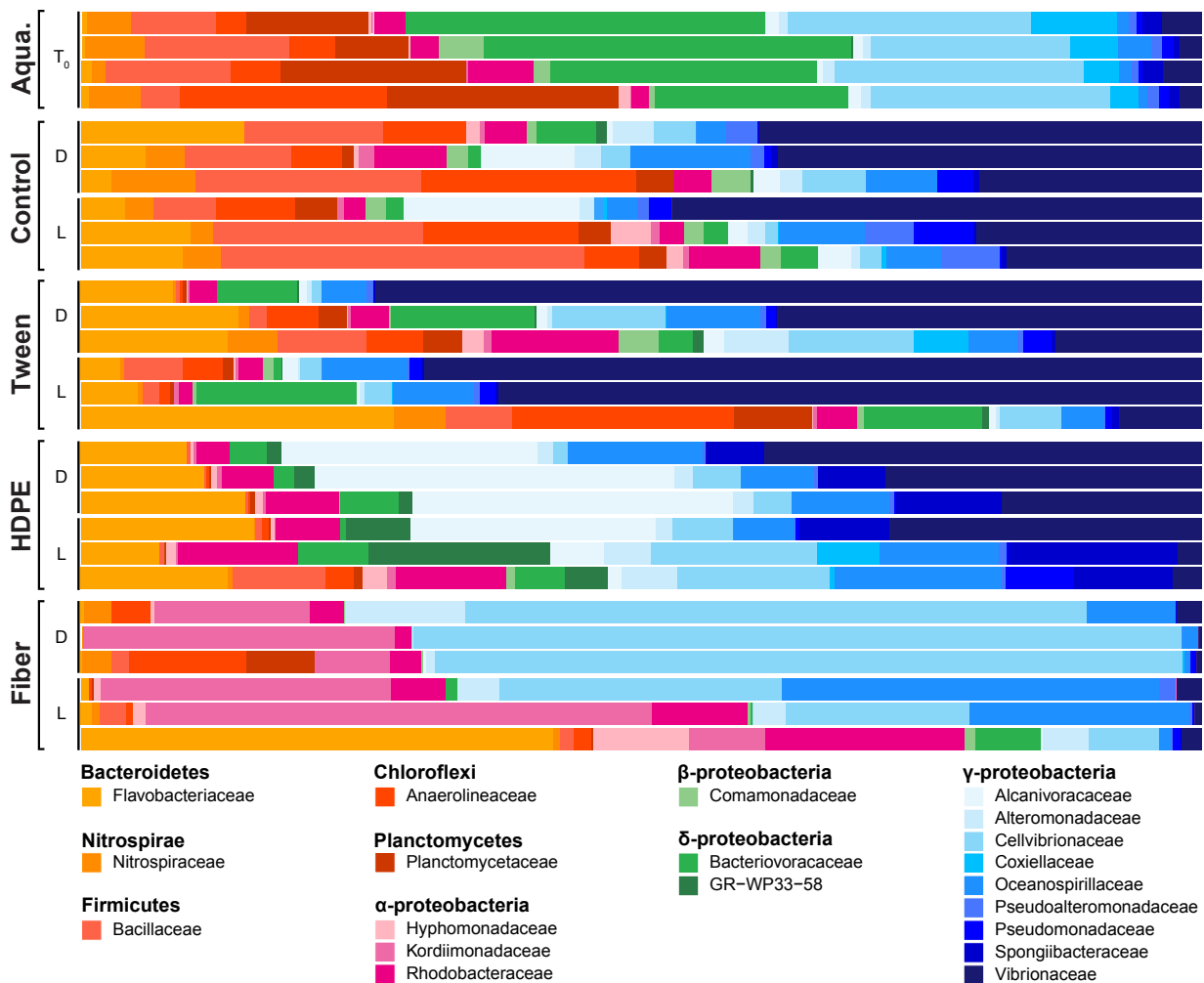


**Figure 5.** The relative proportion of the 20 most abundant families across all incubations, separated into incubation types and light conditions (T<sub>0</sub>: initial community; D: dark; L: light).

295 indicates the development of polymer-dependent taxa, which is also supported by the findings of  
 296 Frère et al. (2018). The families Oceanospirillaceae, Vibrionaceae, Flavobacteriaceae and  
 297 Rhodobacteraceae are putative to the plastisphere with common representatives in HDPE and  
 298 textile fiber incubations, however less diverse than previously observed in other studies<sup>3,5</sup>. This  
 299 might be related to the short experimental time; micropollutants and debris are otherwise  
 300 accumulating over months and years in the ocean<sup>30</sup>.

301 Operational taxonomic units (OTUs) of bacteria that were enriched in particular incubations  
 302 were identified (Fig. 6). Thirty-one OTUs are shared between all incubation types and the  
 303 aquarium water itself, of which two OTUs, i.e., OTU001 ( $\gamma$ -proteobacteria) and OTU004  
 304 (Flavobacteriia), were highly abundant across all incubations (Fig. 6). Only one taxon was  
 305 especially enriched in the tween incubation and shared some OTUs with HDPE and control  
 306 incubations, which were largely affiliated with the  $\gamma$ -proteobacteria. Textile fibers were especially  
 307 colonized by  $\alpha$ - and  $\gamma$ -proteobacteria, identified as first colonizers<sup>6,7</sup>. HDPE incubations were  
 308 mainly characterized by the development of Bacteroidetes (i.e., Family Flavobacteriaceae),  
 309 additionally to  $\alpha$ - and  $\gamma$ -proteobacteria, hypothesized to colonize plastics at a later stage<sup>6,7</sup>.

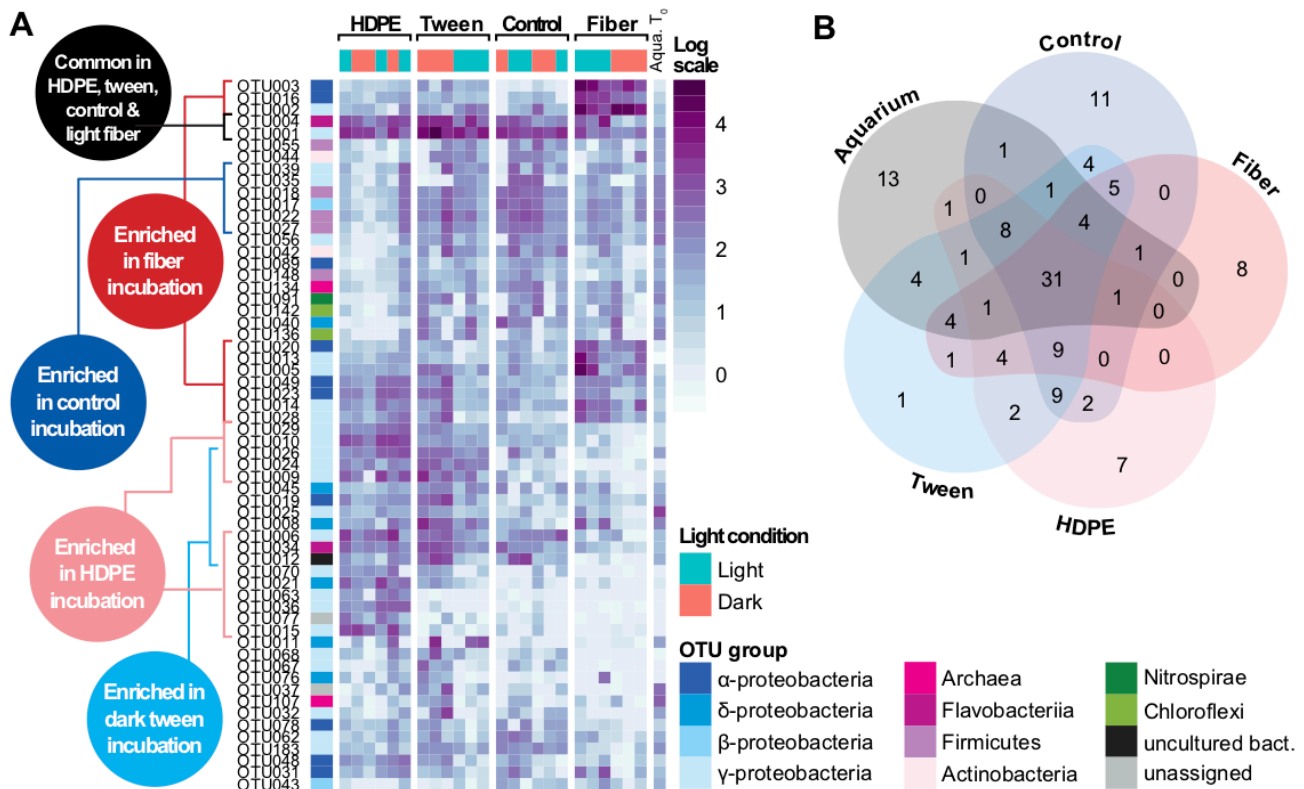


**Figure 6.** A) Log-scaled heat map highlighting the abundance of the 10 most abundant OTUs in each incubation. B) Venn diagram showing a core community, and incubation-specific OTUs.

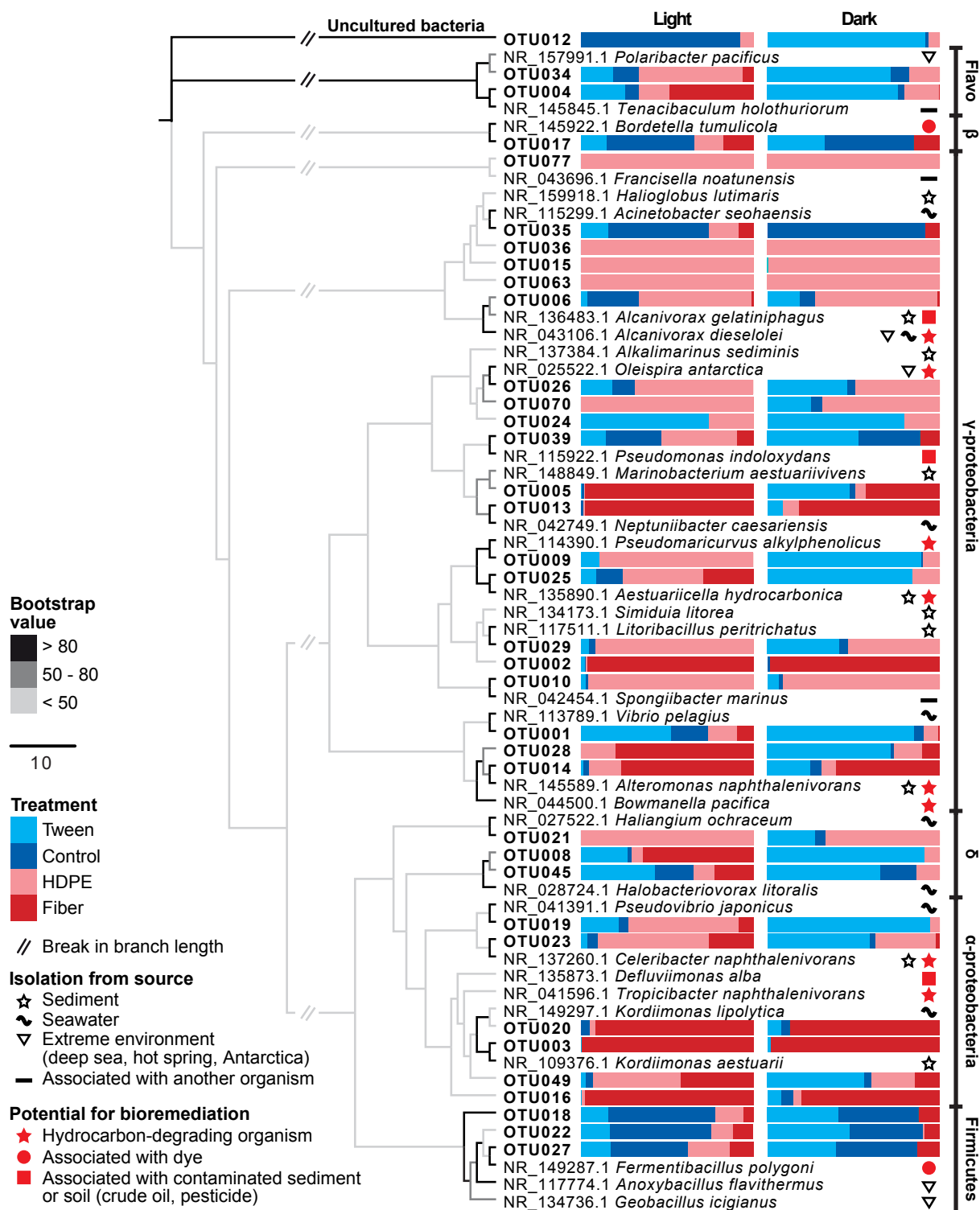


**Figure 7.** Phylogenetic reconstruction of 36 OTUs identified as incubation-enriched in Fig. 6 and their closest associated named species from NCBI database. The relative abundance of OTUs in each incubation (pale blue: tween; dark blue: control; pale red: HDPE; dark red: fiber) is represented by bar charts, divided according to the light condition. Named- species microorganisms were classified based on their isolation from the source (black star, wave, triangle and line) and marked for their potential to bioremediate microplastics (red star, circle and square).

311 **Impact of light on microbial development.** The presence of light was correlated with the  
312 development of unique microbial communities, especially observable in HDPE and textile fiber  
313 incubations, similar to the findings of Fuhrman et al. (2008) and Sánchez et al. (2017) regarding  
314 the impact of light on the microbial communities<sup>31,32</sup>. Indeed, the dark-incubated HDPE microbial  
315 community was dominated by the three families Vibrionaceae, Alcanivoracaceae and  
316 Flavobacteriaceae, whereas the light-grown HDPE microbial community was more diverse with a  
317 shared dominance between eight families (Rhodobacteraceae, GR-WP33-58, Spongiibacteraceae,  
318 Vibrionaceae, Cellvibrionaceae, Oceanospirillaceae, Alcanivoracaceae, and Flavobacteriaceae)  
319 (Fig. 5).

320 Some taxa were enriched under artificial sunlight when incubated with HDPE and textile fibers,  
321 but enriched in the presence of Tween 20 under dark conditions. This observation is well  
322 represented by OTU028 and OTU049, which were most abundant in textile fiber and HDPE  
323 incubations in the presence of light, otherwise dominant in the tween incubation under dark  
324 conditions. In general, OTUs enriched in Tween-20 incubations had a higher relative abundance  
325 in dark settings, also supported by our qPCR results. The flexibility these taxa show in using carbon  
326 from various sources (HDPE microbeads vs Tween 20) depending on the light availability might  
327 highlight an opportunistic behaviour<sup>33</sup>. Another hypothesis suggests a higher level of available  
328 DOC in light-exposed textile fiber and HDPE incubations, caused by the polymer exposure to  
329 artificial sunlight<sup>13,28</sup>. These findings may help us better understand the plastisphere dynamic in  
330 situations similar to, for example, microorganisms settled on plastic debris initially floating in the  
331 photic zone and later buried in the sediment or sinking in regions with limited light availability.

332  
333 **Hydrocarbon-degrading bacteria.** Several OTUs enriched in the different incubation types  
334 revealed to be closely related to known hydrocarbon degrading microorganisms (Fig. 7). This,  
335 together with the increased rates of oxygen consumption in those incubations, highlights their  
336 potential for biodegradation of organic carbon based micropollutants. The six most abundant  
337 OTUs of the textile fiber incubation (OTU002, -003, -005, -013, -016 and -020) are closely related  
338 to the genera *Kordiimonas* and *Defluviimonas* ( $\alpha$ -proteobacteria), and *Simiduila*,  
339 *Marinobacterium* and *Neptuniibacter* ( $\gamma$ -proteobacteria) according to the inferred phylogenetic  
340 tree. OTU003 and -020 were also closely related to *K. gwangyangensis* (NR\_043103.1), which  
341 can hydrolyze six different polycyclic aromatic hydrocarbons (PAHs)<sup>34</sup>, giving this taxon a strong



342 potential for microplastic bioremediation. The genus *Alteromonas*, hosting hydrocarbon-degrading  
343 microorganisms, has been previously identified as part of the plastisphere from North Adriatic Sea  
344 and Atlantic Ocean <sup>5,35</sup>. More specifically, *Alteromonas naphthalenivorans* was identified as a  
345 naphthalene consumer <sup>36</sup>. *Defluviimonas alba* was isolated from an oilfield water sample  
346 suggesting that it has a potential for degradation of hydrocarbon similarly to *Defluviimonas*  
347 *pyrenivorans* <sup>37</sup>, however not tested for hydrocarbon hydrolysis <sup>38</sup>. *Bowmanella pacifica* was  
348 identified during a search for pyrene-degrading bacteria <sup>39</sup>, which is a PAH highly concentrated in  
349 certain plastics <sup>40</sup>. *Bowmanella* spp. were also identified on polyethylene terephthalate (PET)  
350 specific assemblages from Northern European waters <sup>41</sup>. Because these taxa were probably  
351 biofilm-forming microorganisms developed on the surface of textile fibers, it is very likely that  
352 they partly consumed the polymer, an available source of carbon and energy, owing to their  
353 capability to hydrolyze hydrocarbons. Although approximately half of the fibers used in the  
354 experiment were of natural fabric, it has been observed that cotton is a powerful sorbent used to  
355 treat oil spill <sup>42</sup>. The latter suggest that cotton fibers may absorb traces of hydrocarbon present in  
356 the environment <sup>43</sup> and, therefore, provide a source of hydrocarbon for hydrocarbonoclastic  
357 bacteria.

358 The HDPE incubation stimulated the activity and enrichment of six OTUs (OTU001, -004, -006,  
359 -010, -015 and -026) closely related to hydrocarbon-degrading bacteria, different from those  
360 enriched in textile fiber incubations. For instance, OTU006 was affiliated with the genus  
361 *Alcanivorax*, which are specialized in degrading alkanes, especially in contaminated marine  
362 environments <sup>44</sup>. This genus was also identified as being potentially important for PET degradation  
363 in the natural marine environment <sup>41</sup>. All other five OTUs were abundant only in light-grown  
364 HDPE communities, which were affiliated with the taxa *Pseudomericurvus alkylphenolicus*,  
365 *Celeribacter naphthalenivorans*, *Oleispira antarctica*, *Tropicibacter naphthalenivorans*, and  
366 *Aestuariicella hydrocarbonica*. Given their enrichment in the HDPE incubations in the presence  
367 of light, and the increased oxygen consumption relative to the control, it seems likely that these  
368 conditions selected for these specific organisms that were uniquely adept to utilize organic carbon  
369 from the HDPE as a carbon and energy source. This indicates their potential for the bioremediation  
370 of this plastic type. The different respiration rates of HPDE treatment and community assembly  
371 compared to the Tween 20 treatment (an emulsifier for the HDPE microbeads) and demonstrates

372 a unique effect on microbial community formation due to the HDPE itself (as opposed to microbes  
373 that may just be eating the Tween that is coated on the HDPE).

374

375 **Extrapolating from our experiment to the natural environment.** Although this study did not  
376 use “natural” microbial communities from the intertidal habitats from which the textile fibers  
377 derive, it tests for the potential response of microbial communities to widespread micropollutants.  
378 Since the identified hydrocarbonoclastic bacteria in our incubations are also common to both  
379 natural marine sediments and water column<sup>5,34,39,41,44</sup>, this study contributes to the developing  
380 understanding of how hydrocarbon-degrading bacteria utilize various fabric types as a carbon and  
381 energy sources during bioremediation processes. Three main lines of evidence indicate that the  
382 plastics and textile fibers were consumed by hydrocarbon-degrading microorganisms during the  
383 experiment: (1) higher rates of oxygen consumption relative to the control, (2) increased  
384 abundance as indicated by qPCR and (3) the development of unique microbial communities that  
385 form in incubations containing different types of micropollutants. Moreover, the same groups of  
386 hydrocarbonoclastic bacteria found in our study are present in the marine environment. The  
387 findings resulting from this study also demonstrated that light availability is an important factor  
388 shaping hydrocarbon-degrading bacterial communities. We speculate that this is due to  
389 photochemical dissolution of the plastic and textile substrates, which might allow for more readily  
390 bioavailable substrates for the developing biofilms. A deeper study into the topic is necessary to  
391 enlarge our understanding behind microbial adaptation to changing environmental conditions,  
392 including photochemical dissolution of plastic waste.

393

## 394 **ACKNOWLEDGEMENTS**

395 This study was conducted within the frame of the program Lehre@LMU, part of the Geobiology  
396 and Paleobiology section of the Department of Earth and Environmental Sciences, Ludwig-  
397 Maximilians-Universität München. We thank Coral Eye Resort (Marco Segre Reinach) for  
398 providing the textile fibers and the Indonesian authorities for providing the research visa and  
399 permit (research permit holder: Elsa Girard; SIP no.: 97/E5/E5.4/SIP/2019). We are also grateful  
400 for the time Aurèle Vuillemin, Ömer Coskun, Paula R. Ramirez, and Nicola Conci took to help us  
401 in the lab and with the data analysis.

402 This study was funded by Lehre@LMU (project number: S19\_F2.; Studi\_Forscht@GEO), and  
403 to budget funds to WO and GW. GW acknowledges support by LMU Munich's Institutional  
404 Strategy LMUexcellent within the framework of the German Excellence Initiative for aquarium  
405 set-up and maintenance.

406

407

## 408 REFERENCES

409 (1) Scott, G. Polymers in Modern Life. In *Polymers and the Environment*; Scott, G., Ed.; Royal Society of  
410 Chemistry, 1999; pp 1–18.

411 (2) Jambeck, J. R.; Geyer, R.; Wilcox, C.; Siegler, T. R.; Perryman, M.; Andrady, A.; Narayan, R.; Law, K. L.  
412 Plastic Waste Inputs from Land into the Ocean. *Science* **2015**, *347* (6223), 764–768.

413 (3) Frère, L.; Maignien, L.; Chalopin, M.; Huvet, A.; Rinnert, E.; Morrison, H.; Kerninon, S.; Cassone, A.-L.;  
414 Lambert, C.; Reveillaud, J.; et al. Microplastic Bacterial Communities in the Bay of Brest: Influence of Polymer Type  
415 and Size. *Environ. Pollut.* **2018**, *242* (Pt A), 614–625.

416 (4) Summer, W. Microbial Degradation of Plastics. *Anti-Corros. Methods Mater.* **1964**, *11* (4), 19–21.

417 (5) Zettler, E. R.; Mincer, T. J.; Amaral-Zettler, L. A. Life in the “Plastisphere”: Microbial Communities on  
418 Plastic Marine Debris. *Environ. Sci. Technol.* **2013**, *47* (13), 7137–7146.

419 (6) Oberbeckmann, S.; Löder, M. G. J.; Labrenz, M. Marine Microplastic-Associated Biofilms – a Review.  
420 *Environ. Chem.* **2015**, *12* (5), 551–562.

421 (7) Quero, G. M.; Luna, G. M. Surfing and Dining on the “plastisphere”: Microbial Life on Plastic Marine  
422 Debris. *Advances in Oceanography and Limnology* **2017**, *8*(2), 199–207.

423 (8) Krueger, M. C.; Harms, H.; Schlosser, D. Prospects for Microbiological Solutions to Environmental Pollution  
424 with Plastics. *Appl. Microbiol. Biotechnol.* **2015**, *99* (21), 8857–8874.

425 (9) Yoshida, S.; Hiraga, K.; Takehana, T.; Taniguchi, I.; Yamaji, H.; Maeda, Y.; Toyohara, K.; Miyamoto, K.;  
426 Kimura, Y.; Oda, K. A Bacterium That Degrades and Assimilates Poly(ethylene Terephthalate). *Science* **2016**, *351*  
427 (6278), 1196–1199.

428 (10) Lamb, J. B.; Willis, B. L.; Fiorenza, E. A.; Couch, C. S.; Howard, R.; Rader, D. N.; True, J. D.; Kelly, L. A.;  
429 Ahmad, A.; Jompa, J.; et al. Plastic Waste Associated with Disease on Coral Reefs. *Science* **2018**, *359* (6374), 460–  
430 462.

- 431 (11) Dris, R.; Gasperi, J.; Saad, M.; Mirande, C.; Tassin, B. Synthetic Fibers in Atmospheric Fallout: A Source  
432 of Microplastics in the Environment? *Mar. Pollut. Bull.* **2016**, *104* (1-2), 290–293.
- 433 (12) Browne, M. A.; Crump, P.; Niven, S. J.; Teuten, E.; Tonkin, A.; Galloway, T.; Thompson, R. Accumulation  
434 of Microplastic on Shorelines Worldwide: Sources and Sinks. *Environ. Sci. Technol.* **2011**, *45* (21), 9175–9179.
- 435 (13) Zhu, L.; Zhao, S.; Bittar, T. B.; Stubbins, A.; Li, D. Photochemical Dissolution of Buoyant Microplastics to  
436 Dissolved Organic Carbon: Rates and Microbial Impacts. *J. Hazard. Mater.* **2020**, *383*, 121065.
- 437 (14) Pichler, M.; Coskun, Ö. K.; Ortega-Arbulú, A.-S.; Conci, N.; Wörheide, G.; Vargas, S.; Orsi, W. D. A 16S  
438 rRNA Gene Sequencing and Analysis Protocol for the Illumina MiniSeq Platform. *MicrobiologyOpen* **2018**, e00611.
- 439 (15) Coskun, Ö. K.; Pichler, M.; Vargas, S.; Gilder, S.; Orsi, W. D. Linking Uncultivated Microbial Populations  
440 and Benthic Carbon Turnover by Using Quantitative Stable Isotope Probing. *Appl. Environ. Microbiol.* **2018**, *84* (18).  
441 <https://doi.org/10.1128/AEM.01083-18>.
- 442 (16) Edgar, R. Taxonomy Annotation and Guide Tree Errors in 16S rRNA Databases. *PeerJ* **2018**, *6*, e5030.
- 443 (17) R Core Team. *R: A Language and Environment for Statistical Computing*; R Foundation for Statistical  
444 Computing: Vienna, Austria, 2017.
- 445 (18) Gouy, M.; Guindon, S.; Gascuel, O. SeaView Version 4: A Multiplatform Graphical User Interface for  
446 Sequence Alignment and Phylogenetic Tree Building. *Mol. Biol. Evol.* **2010**, *27* (2), 221–224.
- 447 (19) Guindon, S.; Dufayard, J.-F.; Lefort, V.; Anisimova, M.; Hordijk, W.; Gascuel, O. New Algorithms and  
448 Methods to Estimate Maximum-Likelihood Phylogenies: Assessing the Performance of PhyML 3.0. *Syst. Biol.* **2010**,  
449 *59* (3), 307–321.
- 450 (20) Buzzini, P.; Massonnet, G. The Discrimination of Colored Acrylic, Cotton, and Wool Textile Fibers Using  
451 Micro-Raman Spectroscopy. Part 1: In Situ Detection and Characterization of Dyes. *J. Forensic Sci.* **2013**, *58* (6),  
452 1593–1600.
- 453 (21) Bouchard, M.; Rivenc, R.; Menke, C.; Learner, T. Micro-FTIR and Micro-Raman Full Paper Study of Paints  
454 Used by San Francisco. *e-PS* **2009**, *6*, 27–37.
- 455 (22) Dris, R.; Gasperi, J.; Mirande, C.; Mandin, C.; Guerrouache, M.; Langlois, V.; Tassin, B. A First Overview  
456 of Textile Fibers, Including Microplastics, in Indoor and Outdoor Environments. *Environ. Pollut.* **2017**, *221*, 453–  
457 458.
- 458 (23) Andrady, A. L. The Plastic in Microplastics: A Review. *Mar. Pollut. Bull.* **2017**, *119* (1), 12–22.
- 459 (24) Corcoran, P. L.; Biesinger, M. C.; Grifi, M. Plastics and Beaches: A Degrading Relationship. *Mar. Pollut.*  
460 *Bull.* **2009**, *58* (1), 80–84.

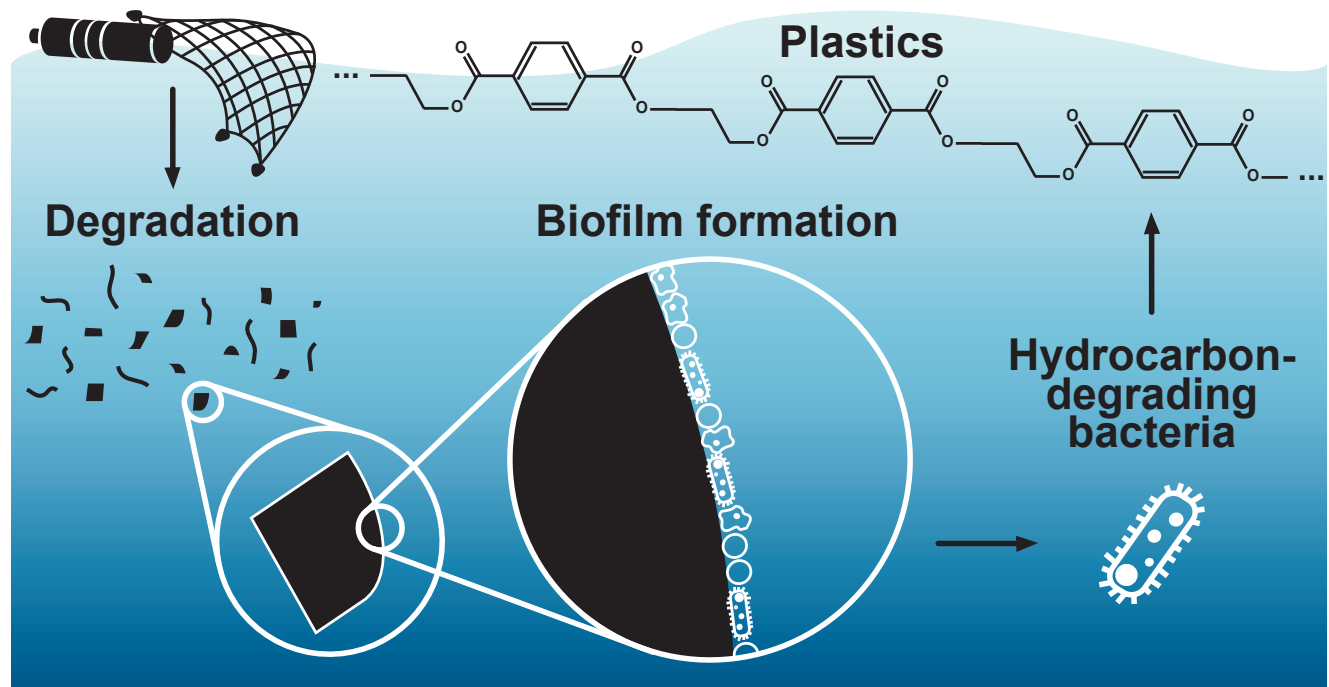
- 461 (25) Barnes, D. K. A.; Galgani, F.; Thompson, R. C.; Barlaz, M. Accumulation and Fragmentation of Plastic  
462 Debris in Global Environments. *Philos. Trans. R. Soc. Lond. B Biol. Sci.* **2009**, *364* (1526), 1985–1998.
- 463 (26) Singh, B.; Sharma, N. Mechanistic Implications of Plastic Degradation. *Polym. Degrad. Stab.* **2008**, *93* (3),  
464 561–584.
- 465 (27) Wilkes, R. A.; Aristilde, L. Degradation and Metabolism of Synthetic Plastics and Associated Products by  
466 *Pseudomonas* Sp.: Capabilities and Challenges. *J. Appl. Microbiol.* **2017**, *123* (3), 582–593.
- 467 (28) Romera-Castillo, C.; Pinto, M.; Langer, T. M.; Álvarez-Salgado, X. A.; Herndl, G. J. Dissolved Organic  
468 Carbon Leaching from Plastics Stimulates Microbial Activity in the Ocean. *Nat. Commun.* **2018**, *9* (1), 1430.
- 469 (29) Patin, N. V.; Pratte, Z. A.; Regensburger, M.; Hall, E.; Gilde, K.; Dove, A. D. M.; Stewart, F. J. Microbiome  
470 Dynamics in a Large Artificial Seawater Aquarium. *Appl. Environ. Microbiol.* **2018**, *84* (10).  
471 <https://doi.org/10.1128/AEM.00179-18>.
- 472 (30) Lebreton, L.; Slat, B.; Ferrari, F.; Sainte-Rose, B.; Aitken, J.; Marthouse, R.; Hajbane, S.; Cunsolo, S.;  
473 Schwarz, A.; Levivier, A.; et al. Evidence That the Great Pacific Garbage Patch Is Rapidly Accumulating Plastic. *Sci.*  
474 *Rep.* **2018**, *8* (1). <https://doi.org/10.1038/s41598-018-22939-w>.
- 475 (31) Fuhrman, J. A.; Schwalbach, M. S.; Stingl, U. Proteorhodopsins: An Array of Physiological Roles? *Nat. Rev.*  
476 *Microbiol.* **2008**, *6* (6), 488–494.
- 477 (32) Sánchez, O.; Koblížek, M.; Gasol, J. M.; Ferrera, I. Effects of Grazing, Phosphorus and Light on the Growth  
478 Rates of Major Bacterioplankton Taxa in the Coastal NW Mediterranean. *Environ. Microbiol. Rep.* **2017**, *9* (3), 300–  
479 309.
- 480 (33) Fredricks, K. M. Adaptation of Bacteria from One Type of Hydrocarbon to Another. *Nature* **1966**, *209*  
481 (5027), 1047–1048.
- 482 (34) Kim, S.-J.; Kwon, K. K. Marine, Hydrocarbon-Degrading Alphaproteobacteria. In *Handbook of*  
483 *Hydrocarbon and Lipid Microbiology*; Timmis, K. N., Ed.; Springer Berlin Heidelberg: Berlin, Heidelberg, 2010; pp  
484 1707–1714.
- 485 (35) Viršek, M. K.; Lovšin, M. N.; Koren, Š.; Kržan, A.; Peterlin, M. Microplastics as a Vector for the Transport  
486 of the Bacterial Fish Pathogen Species *Aeromonas Salmonicida*. *Mar. Pollut. Bull.* **2017**, *125* (1-2), 301–309.
- 487 (36) Jin, H. M.; Kim, K. H.; Jeon, C. O. *Alteromonas Naphthalenivorans* Sp. Nov., a Polycyclic Aromatic  
488 Hydrocarbon-Degrading Bacterium Isolated from Tidal-Flat Sediment. *Int. J. Syst. Evol. Microbiol.* **2015**, *65* (11),  
489 4208–4214.

- 490 (37) Zhang, S.; Sun, C.; Xie, J.; Wei, H.; Hu, Z.; Wang, H. *Defluviimonas Pyrenivorans* Sp. Nov., a Novel  
491 Bacterium Capable of Degrading Polycyclic Aromatic Hydrocarbons. *Int. J. Syst. Evol. Microbiol.* **2018**, 68 (3), 957–  
492 961.
- 493 (38) Pan, X.-C.; Geng, S.; Lv, X.-L.; Mei, R.; Jiangyang, J.-H.; Wang, Y.-N.; Xu, L.; Liu, X.-Y.; Tang, Y.-Q.;  
494 Wang, G.-J.; et al. *Defluviimonas Alba* Sp. Nov., Isolated from an Oilfield. *Int. J. Syst. Evol. Microbiol.* **2015**, 65 (Pt  
495 6), 1805–1811.
- 496 (39) Lai, Q.; Yuan, J.; Wang, B.; Sun, F.; Qiao, N.; Zheng, T.; Shao, Z. *Bowmanella Pacifica* Sp. Nov., Isolated  
497 from a Pyrene-Degrading Consortium. *Int. J. Syst. Evol. Microbiol.* **2009**, 59 (Pt 7), 1579–1582.
- 498 (40) Chen, Q.; Reisser, J.; Cunsolo, S.; Kwadijk, C.; Kotterman, M.; Proietti, M.; Slat, B.; Ferrari, F. F.; Schwarz,  
499 A.; Levivier, A.; et al. Pollutants in Plastics within the North Pacific Subtropical Gyre. *Environ. Sci. Technol.* **2018**,  
500 52 (2), 446–456.
- 501 (41) Oberbeckmann, S.; Loeder, M. G. J.; Gerdts, G.; Osborn, A. M. Spatial and Seasonal Variation in Diversity  
502 and Structure of Microbial Biofilms on Marine Plastics in Northern European Waters. *FEMS Microbiol. Ecol.* **2014**,  
503 90 (2), 478–492.
- 504 (42) Choi, H.-M.; Kwon, H.-J.; Moreau, J. P. Cotton Nonwovens as Oil Spill Cleanup Sorbents. *Text. Res. J.*  
505 **1993**, 63 (4), 211–218.
- 506 (43) Singh, V.; Kendall, R. J.; Hake, K.; Ramkumar, S. Crude Oil Sorption by Raw Cotton. *Ind. Eng. Chem. Res.*  
507 **2013**, 52 (18), 6277–6281.
- 508 (44) Barbato, M.; Scoma, A.; Mapelli, F.; De Smet, R.; Banat, I. M.; Daffonchio, D.; Boon, N.; Borin, S.  
509 Hydrocarbonoclastic *Alcanivorax* Isolates Exhibit Different Physiological and Expression Responses to N-Dodecane.  
510 *Front. Microbiol.* **2016**, 7, 2056.

511

512

## Graphical Abstract



513

514